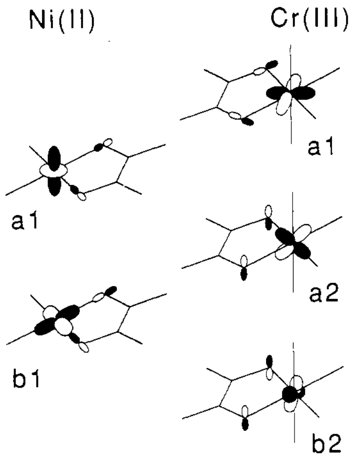

Figure 6. Schematic representation of the magnetic orbitals centered on the Cr(III) ion and the Ni(II) ions in $CrNi_3$.

or not coupled. This difference is emphasized in Figure 5.

Discussion and Conclusion

We want first to turn back to the symmetry considerations and to analyze the nature of the magnetic orbitals involved in the Cr(III)–Ni(II) interactions within $CrNi_3$.

J in (2) refers to a Cr(III)–Ni(II) pair. Therefore, it is justified to consider the symmetry of the Cr(ox)Ni bridging network, close to C_{2v}, instead of the overall symmetry of $CrNi_3$, close to C_{3v}. In this C_{2v} symmetry, the unpaired electrons of Cr(III) occupy orbitals transforming as $a_1 + a_2 + b_2$ and those of Ni(II) orbitals transforming as $a_1 + b_1$. These orbitals are shown in Figure 6. J may be written as a sum of J_{ij}'s contributions involving pairs of interacting orbitals as[1]

$$J = \tfrac{1}{3}(J_{a1a1} + J_{a1b1} + J_{a2a1} + J_{a2b1} + J_{b2}a_1 + J_{b2b1}) \quad (8)$$

In (8), all the J_{ij}'s are positive, since they involve orthogonal orbitals, except J_{a1a1}. This contribution, however, may be expected to be rather small. Indeed, the $a_1(z^2)$ orbital centered on nickel is weakly delocalized in the plane of the oxalato bridge. Among the positive contributions, J_{a1b1} is certainly the most important since the a_1 orbital centered on chromium and the b_1 orbital centered on nickel are both situated in the plane of the bridging network and may efficiently interact. It can be noticed here that the interaction between Cu(II) and VO^{2+} ions through the oxalato ligand in (tmen)Cu(ox)VO(ox) with tmen = *N,N,N′,N′*-tetramethylethylenediamine also involves orthogonal b_1 and a_1 magnetic orbitals.[21] The interaction parameter J, however, has been found to be almost negligible ($J < 1$ cm^{-1}). The more efficient character of the ferromagnetic exchange pathway in $CrNi_3$ could be due to the fact that the a_1 magnetic orbital around Cr(III) would be more delocalized toward the oxygen atoms of the bridge than the a_1 magnetic orbital of VO^{2+}. Indeed, Cr(III) is certainly located in the plane of the oxalato bridge whereas the V(IV) ion is pulled out of this plane toward the oxygen atom of the vanadyl group.

To conclude, we recall that one of our goals is to design molecular-based ferromagnets.[10,11] Our strategy along this line consists of synthesizing high-spin molecules or chains and then assembling them in a ferromagnetic fashion within the crystal lattice. To obtain high-spin molecules, we are exploring two different approaches. The former is the achieving of ferromagnetic interactions due to the orthogonality of the magnetic orbitals. $CrNi_3$ provides a spectacular example of the possibilities of this approach. A $S = {}^9/_2$ ground state, if no longer unique,[22–24] is still quite unusual. The latter strategy consists of polarizing high peripheral spins due to antiferromagnetic interactions with a small central spin. We have attempted to apply this approach by using manganese(II) instead of nickel(II) in the synthesis process in order to obtain $CrMn_3$. Since the Cr(III)–Mn(II) interaction is expected to be antiferromagnetic,[1–4] the ground state of $CrMn_3$ would be characterized by the spin $S = 3S_{Mn} - S_{Cr} = 6$. Unfortunately, we have not yet succeeded in synthesizing such a compound.

Registry No. **1**, 14217-01-7; **2**, 117686-66-5; $CrNi_3$, 117709-37-2; $[Ni(Me_6\text{-}[14]\text{-}ane\text{-}N_4)](ClO_4)_2$, 52553-45-4.

---

(21) Julve, M.; Verdaguer, M.; Charlot, M. F.; Kahn, O.; Claude, R. *Inorg. Chim. Acta* **1984**, *82*, 5.
(22) Bencini, A.; Benelli, C.; Caneschi, A.; Carlin, R. L.; Dei, A.; Gatteschi, D. *J. Am. Chem. Soc.* **1985**, *107*, 8128.
(23) Bencini, A.; Benelli, C.; Caneschi, A.; Dei, A.; Gatteschi, D. *Inorg. Chem.* **1986**, *25*, 572.
(24) Pei, Y.; Journaux, Y.; Kahn, O. *Inorg. Chem.* **1988**, *27*, 399.

Contribution from the Department of Applied Chemistry, Faculty of Engineering, Kumamoto University,
Kurokami, Kumamoto 860 Japan, and Institute for Molecular Science, Myodaiji, Okazaki 444, Japan

Electronic Structure and Enhanced Reactivity of Carbon Dioxide Coordinated with a Rhodium(I) Complex. An ab Initio MO Study

Shigeyoshi Sakaki,*[1a] Tetsuro Aizawa,[1a] Nobuaki Koga,[1b] Keiji Morokuma,[1b] and Katsutoshi Ohkubo[1a]

Received June 7, 1988

An ab initio MO study has been carried out on $RhCl(AsH_3)_4(CO_2)$ and the isolobal adduct $(NH_3)(CO_2)$. Although $RhCl(AsH_3)_4(CO_2)$ has a pseudooctahedral structure with a $4d^8$ electron configuration, the most stable state is calculated to be a singlet. This result agrees well with the experimentally reported diamagnetism. The reactivity of carbon dioxide for electrophilic attack is predicted to be much more enhanced in $RhCl(AsH_3)_4(CO_2)$ than in $(NH_3)(CO_2)$, which is rationalized in terms of the coordinate bonding nature of carbon dioxide. The coordinate bond of CO_2 to $RhCl(AsH_3)_4$ is described by three-orbital mixing of Rh d_{z^2} and CO_2 π and π^* orbitals; the main interaction is a charge transfer from the Rh d_{z^2} to the CO_2 π^* orbital, into which the CO_2 π orbital mixes in an antibonding fashion with the Rh d_{z^2} orbital. This orbital mixing accumulates the electron population on the O atom of CO_2, raises the CO_2 π and nonbonding π orbital energies, and increases the O p_π contribution in the HOMO. All of these results enhance the reactivity of CO_2 with electrophiles.

Introduction

There has been much current interest in the fixation of carbon dioxide into organic substances.[2] During the last decade, intensive efforts have been devoted to the preparation and the characterization of transition-metal carbon dioxide complexes,[3–10] because

---

(1) (a) Kumamoto University. (b) Institute for Molecular Science.
(2) For example, (a) Sneeden, R. P. A. *Comprehensive Organometallic Chemistry*; Wilkinson, G., Ed.; Pergamon Press: Oxford, England, 1982; Vol. 8. (b) Palmer, D. A.; Van Eldik, R. *Chem. Rev.* **1983**, *83*, 651. (c) Darensbourg, D. J.; Kudaroski, R. A. *Adv. Organomet. Chem.* **1983**, *22*, 129.
(3) (a) Floriani, C.; Fachinetti, G. *J. Chem. Soc., Chem. Commun.* **1974**, 615. (b) Fachinetti, G.; Floriani, C.; Zanazzi, P. F. *J. Am. Chem. Soc.* **1978**, *100*, 7405. (c) Gambarotta, S.; Arena, F.; Floriani, C.; Zanazzi, P. F.; *Ibid.* **1982**, *104*, 5082.
(4) (a) Aresta, M.; Nobile, C. F.; Albano, V. G.; Forni, E.; Manassero, M. *J. Chem. Soc., Chem. Commun.* **1975**, 636. (b) *Inorg. Chim. Acta* **1977**, *24*, L49. (c) *J. Chem. Soc., Dalton Trans.* **1977**, 708.

0020-1669/89/1328-0103$01.50/0

Chart I

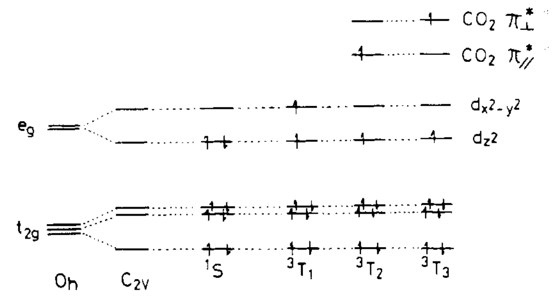

[a] See Reference 37 for these notations.

formation of transition-metal complexes is believed to be one of the most powerful and universal ways of activating inert molecules. In several pioneering studies, fixation of carbon dioxide with transition-metal complexes has succeeded.[11-24] However, some difficulties are still found; for instance, only a limited number of metal complexes can be used for coordination of carbon dioxide, and catalytic fixation of carbon dioxide into organic substances is not yet easy.

In this light, it is worthwhile to investigate the electronic structure and reactivity of carbon dioxide coordinated to transition-metal complexes. Molecular orbital methods are expected to be effective in such investigation, and several MO studies of transition-metal carbon dioxide complexes have been reported.[25,26]

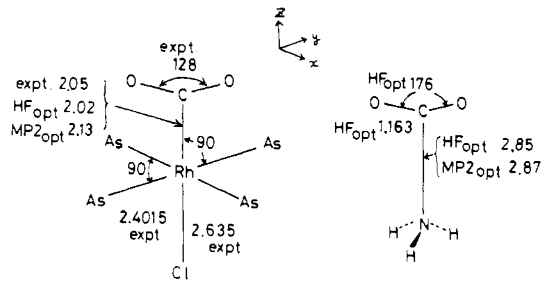

Figure 1. Geometries of the complexes examined: partially optimized structure of $RhCl(AsH_3)_4(CO_2)$ and optimized structure of $(NH_3)(CO_2)$.

However, little work has been performed to investigate how much carbon dioxide is activated by coordination to transition-metal complexes.

In this work, the electronic structure of a pseudooctahedral η^1-C-coordinated carbon dioxide complex, $RhCl(AsH_3)_4(CO_2)$, is studied with an ab initio MO method. This complex is an interesting subject for a theoretical study from the following points of view: (1) diamagnetism has been reported for this complex,[27] although a d–d triplet state generally is expected to be the ground state for a pseudooctahedral complex with a d^8 electron configuration, as shown in Chart I, and (2) enhancement of electrophilic attack to carbon dioxide has been predicted in this complex[5b] as well as in a similar η^1-C-coordinated carbon dioxide complex, $IrCl(dmpe)_2(CO_2)$.[28] MO calculations were also carried out on $RhCl(AsH_3)_4(NH_3)$ and a van der Waals complex, $(NH_3)(CO_2)$, to clarify characteristics of transition-metal carbon dioxide complexes by comparing $RhCl(AsH_3)_4(CO_2)$ with these complexes. Through this theoretical study, we hope (a) to elucidate why the ground state of $RhCl(AsH_3)_4(CO_2)$ is a singlet, in spite of its pseudooctahedral $4d^8$ electron configuration, (b) to characterize the carbon dioxide ligand by comparing it with the usual NH_3 ligand, (c) to investigate differences between the charge-transfer type complex, $RhCl(AsH_3)_4(CO_2)$, and the van der Waals complex, $(NH_3)(CO_2)$, and (d) to assess how much carbon dioxide is activated toward electrophilic attack in $RhCl(AsH_3)_4(CO_2)$ and $(NH_3)(CO_2)$ and to elucidate the origin of the activation.

Computational Details

The standard ab initio closed-shell Hartree–Fock (HF) calculations were carried out on singlet states of $RhCl(AsH_3)_4(CO_2)$, $RhCl(AsH_3)_4(NH_3)$, and $(NH_3)(CO_2)$ with the GAUSSIAN 82 program,[29] and ab initio unrestricted Hartree–Fock (UHF) calculations were performed on triplet states of $RhCl(AsH_3)_4(CO_2)$ and $RhCl(AsH_3)_4(NH_3)$. Further, MP2 calculations were carried out on these complexes with a frozen-core approximation, by using molecular orbitals attained above. We recognize that the singlet state calculated with the RHF method can not be compared in general with the triplet state calculated with the UHF method. As will be shown later, however, the singlet state of $RhCl(AsH_3)_4(CO_2)$ is calculated to be much more stable (>30 kcal/mol) than the triplet state. The general trend for the introduction of the electron correlation effect is that it stabilizes the closed-shell RHF state more than the open-shell UHF state. Actually, as will be shown later as well, the RMP2 calculation for the singlet state and the UMP2 calculation for the triplet state increase the relative stability of the singlet. Therefore, we may conclude that the full account of the electron correlation effect is not likely to change the ordering of the two states and that the relative stabilities of the singlet and triplet states would be reasonably accounted for in calculations based on RHF, RMP2, UHF, and UMP2 methods.

---

(5) (a) Herskovitz, T.; Guggenberger, L. J. *J. Am. Chem. Soc.* **1976**, *98*, 1615. (b) Calabrese, J. C.; Herskovitz, T.; Kinney, J. B. *Ibid.* **1983**, *105*, 5914.

(6) Bristow, G. S.; Hitchcock, P. B.; Lappert, M. F. *J. Chem. Soc., Chem. Commun.* **1981**, 1145.

(7) Mason, M. G.; Ibers, J. A. *J. Am. Chem. Soc.* **1982**, *104*, 5153.

(8) Maher, J. M.; Lee, G. R.; Cooper, N. J. *J. Am. Chem. Soc.* **1982**, *104*, 6797.

(9) Alvarez, R.; Carmona, E.; Poveda, M.; Sanchez-Delgado, R. *J. Am. Chem. Soc.* **1984**, *106*, 2731. Alvarez, R.; Carmona, E.; Marin, J. M.; Poveda, M. L.; Gutierrez-Puebla, E.; Monge, A. *Ibid.* **1986**, *108*, 2286.

(10) Bianchini, C.; Meli, A. *J. Am. Chem. Soc.* **1984**, *106*, 2698.

(11) Beverwijk, C. D. M.; Van der Kerk, G. J. M. *J. Organomet. Chem.* **1973**, *49*, C59.

(12) (a) Pu, L. S.; Yamamoto, A.; Ikeda, S. *J. Am. Chem. Soc.* **1968**, *90*, 3896. (b) Komiya, S.; Yamamoto, A. *J. Organomet. Chem.* **1972**, *46*, C58. (c) Ikariya, T.; Yamamoto, A. *Ibid.* **1974**, *72*, 145. (d) Miyashita, A.; Yamamoto, A. *Ibid.* **1976**, *113*, 187. (e) Komiya, S.; Yamamoto, A. *Bull. Chem. Soc. Jpn.* **1976**, *49*, 784.

(13) Koinuma, H.; Yoshida, Y.; Hirai, H. *Chem. Lett.* **1975**, 1223.

(14) (a) Inoue, S.; Sasaki, Y.; Hashimoto, H. *J. Chem. Soc., Chem. Commun.* **1975**, 718; *Chem. Lett.* **1976**, 863. (b) Inoue, S.; Takeda, N. *Bull. Chem. Soc. Jpn.* **1977**, *50*, 984. (c) Kojima, F.; Aida, T.; Inoue, S. *J. Am. Chem. Soc.* **1986**, *108*, 391.

(15) Fruge, D. R.; Fong, G. D.; Fong, F. K. *J. Am. Chem. Soc.* **1979**, *101*, 3694.

(16) (a) Fisher, B.; Eisenberg, R. *J. Am. Chem. Soc.* **1980**, *102*, 7363. (b) Beley, M.; Colin, J. P.; Ruppert, R.; Sauvage, J. P. *J. Chem. Soc., Chem. Commun.* **1984**, 1315.

(17) (a) Darensbourg, D. J.; Rohichi, A.; Darensbourg, M. Y. *J. Am. Chem. Soc.* **1981**, *103*, 3223. (b) Darensbourg, D. J.; Ovalles, C. *J. Am. Chem. Soc.* **1984**, *106*, 3750. (c) Darensbourg, D. J.; Hanckel, R. K.; Bauch, C. G.; Pala, M.; Simmons, D.; White, J. N. *Ibid.* **1985**, *107*, 7463. (d) Darensbourg, D. J.; Grötsch, G. *Ibid.* **1985**, *107*, 7473. (e) Darensbourg, D. J.; Ovalles, C. *Inorg. Chem.* **1986**, *25*, 1603.

(18) Bodnar, T.; Coman, E.; Menard, K.; Cutler, A. *Inorg. Chem.* **1982**, *21*, 1275.

(19) Lieber, C. M.; Lewis, N. S. *J. Am. Chem. Soc.* **1984**, *106*, 5033.

(20) Bianchini, C.; Ghilardi, C. A.; Meli, A.; Medollini, S.; Orlandini, A. *Inorg. Chem.* **1985**, *24*, 924.

(21) Cocolios, P.; Guilard, R.; Bayeul, D.; Lecomte, C. *Inorg. Chem.* **1985**, *24*, 2058.

(22) Alvarez, R.; Carmona, E.; Cole-Hamilton, D. J.; Galindo, A.; Gutierrez-Puebla, E.; Monge, A.; Poveda, M. L.; Ruiz, C. *J. Am. Chem. Soc.* **1985**, *107*, 5529.

(23) Gambarotta, S.; Strologo, S.; Floriani, C.; Chiesi-Villa, A.; Guastini, C. *J. Am. Chem. Soc.* **1985**, *107*, 6278.

(24) Lee, G. R.; Maher, J. M.; Cooper, N. J. *J. Am. Chem. Soc.* **1987**, *109*, 2956.

(25) (a) Sakaki, S.; Kudou, N.; Ohyoshi, A.; *Inorg. Chem.* **1977**, *16*, 202. (b) Sakaki, S.; Kitaura, K.; Morokuma, K. *Ibid.* **1982**, *21*, 760. (c) Sakaki, S.; Dedieu, A. *J. Organomet. Chem.* **1986**, *314*, C63. (d) *Inorg. Chem.* **1987**, *26*, 3278.

(26) Mealli, C.; Hoffmann, R.; Stockis, A. *Inorg. Chem.* **1984**, *23*, 56.

(27) Ittel, S. D.; Herskovitz, T. Private communication. This complex is diamagnetic at room temperature.

(28) Harlow, R. L.; Kinney, J. B.; Herskovitz, T. *J. Chem. Soc., Chem. Commun.* **1980**, 813.

(29) Binkley, J. S.; Frisch, M.; Reghavachari, K.; DeFrees, D.; Schlegel, H. B.; Whiteside, R.; Fluder, E.; Seeger, R.; Pople, J. A., Carnegie-Mellon Quantum Chemistry Archive, Carnegie-Mellon University, Pittsburgh, PA, 1983. This program is implemented with the effective core potential program of L. R. Kahn by N. Koga and K. Morokuma.

Table I. Comparison of Several Spin States of $RhCl(AsH_3)_4(CO_2)$, $RhCl(AsH_3)_4(NH_3)$, and $RhCl(AsH_3)_4$ (Energies in kcal/mol)

		$RhCl(AsH_3)_4(CO_2)$				$RhCl(AsH_3)_4(NH_3)$		$RhCl(AsH_3)_4$	
		^1S	$^3T_1$	$^3T_2$	$^3T_3$	^1S	$^3T_1$	^1S	$^3T_1$
ΔE	HF	0.0^b	31.2	46.4	124.9	0.0^d	−48.0	0.0^f	−1.9
	MP2	0.0^c	53.4			0.0^e	−33.2	0.0^g	9.7
INT	HF	55.7^h	14.5^i						
	MP2	65.7	22.0						
DEF	HF	57.5^j	57.5^j						
	MP2	38.6	38.6						
BE	HF	-1.8^k	-42.9^l			-42.5^k	5.6^l		
	MP2	27.0	−16.6			−37.4	−4.3		

[a] See Chart I for notations of spin states. R(Rh–C) = 2.02 Å and R(Rh–N) = 2.23 Å. [b] −254.7145 au. [c] −255.5155 au. [d] −123.4336 au. [e] −123.9614 au. [f] −67.3996 au. [g] −67.4154 au. [h] Interaction energy (INT) = $E_t(L_{dist}) + E_t[RhCl(AsH_3)_4{:}(^1S)] - E_t[RhCl(AsH_3)_4L{:}(^1S)]$, where "dist" means the distorted structure taken in the Rh(I) complex and L is either CO_2 or NH_3. [i] Interaction energy (INT) = $E_t(L_{dist}) + E_t[RhCl(AsH_3)_4{:}(^3T_1)] - E_t[RhCl(AsH_3)_4L{:}(^3T_1)]$ where "dist" means the distorted structure taken in the Rh(I) complex and L is either CO_2 or NH_3. [j] Deformation energy (DEF) = $E_t(L_{dist}) - E_t(L_{eq})$. [k] Binding energy (BE) = $E_t(L_{eq}) + E_t[RhCl(AsH_3)_4{:}(^1S)] - E_t[RhCl(AsH_3)_4L{:}(^1S)]$, where "eq" means the equilibrium structure and L is either CO_2 or NH_3. [l] Binding energy (BE) = $E_t(L_{eq}) + E_t[RhCl(AsH_3)_4{:}(^3T_1)] - E_t[RhCl(AsH_3)_4L{:}(^3T_1)]$, where "eq" means the equilibrium structure and L is either CO_2 or NH_3.

A (3s 3p 4d) primitive set, contracted to a [2s 2p 2d] set, was used to represent the 4d, 5s, and 5p orbitals of Rh.[30] Primitive sets of (3s 3p), contracted to [2s 2p] sets, were employed to represent the *n*s and *n*p valence orbitals of Cl and As (n = 3 for Cl and 4 for As).[31] The [Kr] core of Rh was replaced by a relativistic effective core potential (ECP) proposed by Hay.[30] The [Ne] core of Cl and the [Ar] core of As were replaced by ECP's.[31] For C, N, and O atoms, MIDI-4 sets were used.[32] Standard (3s) and (4s) primitives, contracted to minimal and [2s] sets, were employed for the H atoms of AsH_3 and NH_3, respectively,[33] in which the scaling factor was taken to be 1.188 for the former and 1.20 for the latter, respectively. The d-polarization function ($\zeta = 0.879$)[32] was added to the basis set of the N atom only in the case of $(NH_3)(CO_2)$.

The geometry of $RhCl(AsH_3)_4(CO_2)$ was taken from the experimental structure of $RhCl(diars)_2(CO_2)$ (diars = *o*-phenylenebis(dimethylarsine)),[3b,5a] while the structure of AsH_3 was assumed to be the same as the experimental structure of the free AsH_3 molecule.[34] Only the Rh–C distance was roughly optimized with parabolic fitting of total energies, keeping the structure of CO_2 fixed. We also tried to optimize the Rh–N distance in $RhCl(AsH_3)_4(NH_3)$ on HF and MP2 levels, in which the structure of the $RhCl(AsH_3)_4$ moiety and that of the NH_3 ligand were assumed to be the same as the structure in $RhCl(AsH_3)_4(CO_2)$ and the experimental structure of the free NH_3 molecule, respectively. However, the total energy decreases monotonously with a lengthening of the Rh–N distance in the range of the usual coordinate bond distance (Rh–N = 1.9–2.35 Å). The Rh–N distance in $RhCl(AsH_3)_4(NH_3)$ was, therefore, rather arbitrarily taken to be 2.23 Å from the experimental structure of $[RhCl(NH_3)_5]^{2+}$.[34]

The geometry of $(NH_3)(CO_2)$ was optimized with the energy gradient method at the Hartree–Fock level. At the MP2 level, only the N–C distance was reoptimized with parabolic fitting of total energies, keeping the other geometrical parameters fixed. The geometries of the complexes examined are shown in Figure 1.

Results and Discussion

Binding Energy of CO_2 Coordination. The Rh–C distance was optimized on the ^1S state, since this electron configuration is calculated to be a ground state, as described later. The optimized value (2.02 Å) at the HF level agrees well with the experimental value (2.05 Å). Introducing the electron correlation effect at the MP2 level slightly lengthens it to 2.13 Å. The interaction energy (INT) of CO_2 coordination, which is defined as a stabilization energy relative to the distorted structure of CO_2, is calculated to be 56 kcal/mol at the HF level and 66 kcal/mol at the MP2 level, as shown in Table I. This difference in INT between HF and MP2 levels does not seem significant. However, introducing electron correlation effects significantly influences the binding energy (BE), which is a stabilization relative to the equilibrium structure of CO_2: BE = −2 kcal/mol at the HF level and +27 kcal/mol at the MP2 level.[35] Also, deformation energy (DEF), which is defined as the destabilization energy required to distort CO_2 from its equilibrium structure to the distorted one in the Rh(I) complex, substantially depends on electron correlation effects: DEF = 58 kcal/mol at the HF level and 39 kcal/mol at the MP2 level. This large electron correlation effect on DEF seems to be a main contributor of the electron correlation effects on BE (note the BE is represented as a difference between INT and DEF; BE = INT − DEF).

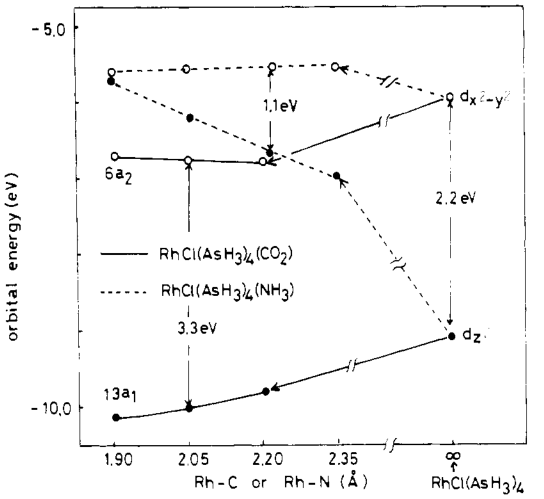

Figure 2. Energy levels of the Rh d_{z^2} and $d_{x^2-y^2}$ orbitals obtained with the UHF-MO calculations for the $^3T_1$ state.

In $RhCl(AsH_3)_4(NH_3)$, however, the optimized bond distance was not found for the Rh–NH_3 bond, as described above, where the optimization was tried on the $^3T_1$ state (vide infra). Furthermore, the BE calculated is very small (see Table I).[35] Thus, further optimization was stopped and $RhCl(AsH_3)_4(NH_3)$ is considered here a model compound to be compared with $RhCl(AsH_3)_4(CO_2)$ (note that our purpose is not to carry out exact investigation of $RhCl(AsH_3)_4(NH_3)$ but to clarify characteristics of $RhCl(AsH_3)_4(CO_2)$ by comparing these two complexes).

Spin States of $RhCl(AsH_3)_4(CO_2)$ and $RhCl(AsH_3)_4(NH_3)$. The lowest singlet and several triplet states are compared in Table I. In $RhCl(AsH_3)_4(CO_2)$, the singlet ^1S state [$(d_{z^2})^2$; see Chart I] is the most stable and a d–d triplet $^3T_1$ [$(d_{z^2})^1(d_{x^2-y^2})^1$] state is significantly less stable than the ^1S state by over 30 kcal/mol.[36]

---

(30) Hay, P. J.; Wadt, W. R. *J. Chem. Phys.* **1985**, *82*, 270.

(31) Wadt, W. R.; Hay, P. J. *J. Chem. Phys.* **1985**, *82*, 284.

(32) Tatewaki, H.; Huzinaga, S. *J. Comput. Chem.* **1980**, *1*, 205.

(33) (a) Van Duijneveldt, F. B. Gaussian Basis Sets for the Atoms H-Ne for use in Molecular Calculations. *IBM J. Res. Dev.* **1971**, 945. (b) Dunning, T. H.; Hay, P. J. *Methods of Electronic Structure Theory*; Schaefer, H. F., Ed.; Plenum Press: New York, 1977; p 1.

(34) Sutton, L. E., Ed. *Tables of Interatomic Distances and Configuration in Molecules and Ions*; Special Publication 11; The Chemical Society: London, 1958.

(35) The BE values described were estimated without taking into account the basis set superposition error (BSSE) and the geometrical relaxation of $RhCl(AsH_3)_4$. The BE value would be reduced considerably by correction of these two factors; for instance, the BSSE value was estimated to be about 5–10 kcal/mol in a similar η^1-C-coordinated CO_2 complex, $[Co(alcn)_2(CO_2)]^-$ (alcn = $HNCHCHCHO^-$), where rather small basis sets were used.[25d]

Table II. Mulliken Populations of $RhCl(AsH_3)_4(CO_2)$ and Its NH_3 Analogue[a,b]

	$RhCl(AsH_3)_4(CO_2)$		$RhCl(AsH_3)_4(NH_3)$		$(NH_3)(CO_2)$
	^1S	$^3T_1$	^1S	$^3T_1$	^1S
Rh d_{z^2}	1.45 (−0.50)[c]	0.91 (−0.22)[d]	0.69 (−0.06)[c]	1.20 (0.07)[d]	7.98 (0.02) (N)
CO_2 or NH_3	22.53 (0.53)	22.33 (0.33)	9.96 (−0.04)	9.91 (−0.09)	22.017 (0.017) (CO_2)
C	5.37 (0.05)	5.43 (0.12)			5.30 (−0.03)
O	8.58 (0.24)	8.45 (0.11)			8.36 (0.02)

[a] R(Rh–C) = 2.02 Å, R(Rh–N) = 2.23 Å, and R(N–C) = 2.87 Å. [b] Values in parentheses are changes in Mulliken population upon coordination of CO_2 or NH_3. Positive values mean an increase and negative values mean a decrease. [c] Referenced to the ^1S state of $RhCl(AsH_3)_4$. [d] Referenced to the $^3T_1$ state of $RhCl(AsH_3)_4$.

Chart II

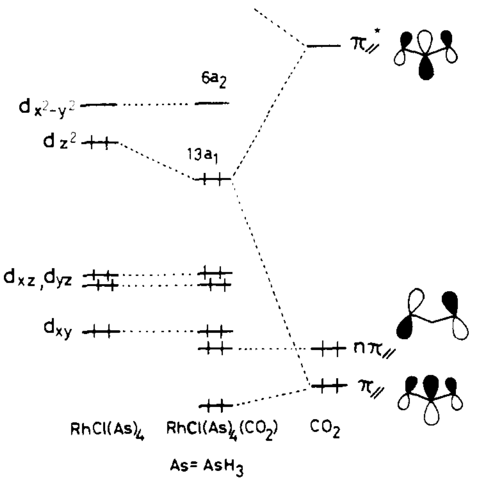

Chart III

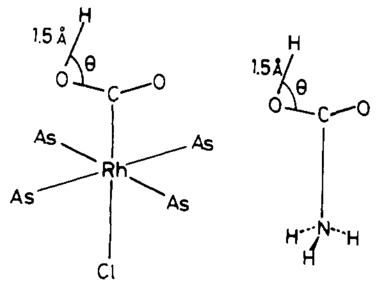

The electron correlation effect at the MP2 level lowers the singlet state more than the triplet, as one would expect. The other types of triplet, $^3T_2$ $[(d_{z^2})^1(CO_2\ \pi_{\parallel}^*)^1]$ and $^3T_3$ $[(d_{z^2})^1(CO_2\ \pi_{\perp}^*)^1]$ (the $\pi_{\parallel}^*$ is on the plane consisting of Rh and CO_2, and the $\pi_{\perp}^*$ is perpendicular to this plane),[37] which arise from electron configuration of the charge-transfer type, are also much less stable at the Hartree–Fock level (further MP2 calculations were not carried out for these states, because introduction of the electron correlation effect is expected to stabilize the singlet state more than the triplet state as described above). These results agree well with the experimentally reported diamagnetism of $RhCl(diars)_2(CO_2)$.[27] In $RhCl(AsH_3)_4(NH_3)$, on the other hand, the $^3T_1$ state is much more stable than the ^1S state at both the HF and the MP2 levels, which agrees with our general expectation that a pseudooctahedral complex tends to have the d–d triplet ground state when a central metal has a d^8 electron configuration, in particular for 3d elements.

The difference in energy between Rh d_{z^2} and $d_{x^2-y^2}$ orbitals is considered one of the key factors for the relative stability of ^1S and $^3T_1$ states. The energy levels of these orbitals are obtained from the UHF calculations of the $^3T_1$ state, in $RhCl(AsH_3)_4(CO_2)$, its NH_3 analogue, and the uncoordinated $RhCl(AsH_3)_4$ (see Figure 2). The uncoordinated $RhCl(AsH_3)_4$ exhibits a moderate difference in energy between these two orbitals. As shown in Table I, the relative energies of ^1S and $^3T_1$ are close to each other, and there is a change in the order upon going from HF to MP2. We will not pursue this inversion, since we are not concerned with the spin multiplicity of the uncoordinated $RhCl(AsH_3)_4$ but with changes in d orbital energies upon coordination of CO_2 and NH_3. Coordination of carbon dioxide with $RhCl(AsH_3)_4$ causes significant mixing of Rh d_{z^2} and CO_2 $\pi_{\parallel}^*$ orbitals, to form the 13a$_1$ orbital, as shown in Chart II. This significant mixing is reflected in the Mulliken populations given in Table II.[38] In the ^1S state, coordination of carbon dioxide remarkably decreases the electron population of the Rh d_{z^2} orbital and substantially increases the

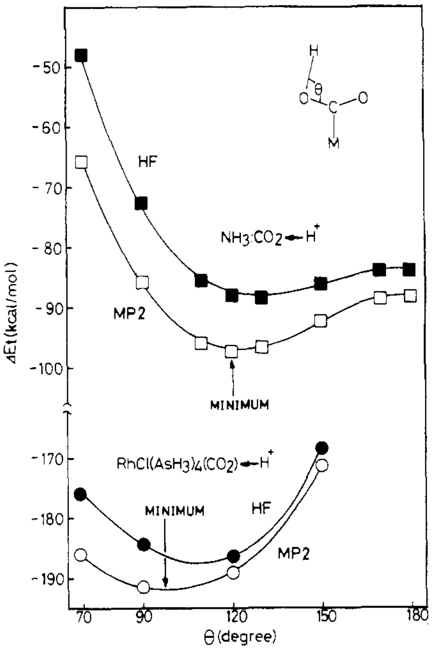

Figure 3. Stabilization in energy caused by H^+ attack to coordinated CO_2. R(Rh–C) = 2.02 Å (experimental).

---

(36) The structure of a compound depends on the spin state, in general. To get a correct energy difference between the singlet and triplet states, optimization must be carried out on both states. Here, however, we are interested in the nature of the electronic structure for the X-ray experimental geometry of $RhCl(diars)_2(CO_2)$ and we have not performed full geometry optimization. In a preliminary optimization at the UHF/MP2 level, the total energy of the triplet state was found to decrease monotonously as the Rh–CO_2 distance increases from 1.9 to 2.2 Å. This suggests that the triplet state is unbound for CO_2 coordination (at 2.35 Å, the total energy increases, due to contamination of higher spin states).

(37) The π and π^* orbitals that are on the plane consisting of the Rh and CO_2 moieties are denoted as the $\pi_{\parallel}$ and $\pi_{\parallel}^*$ orbitals. The other π and π^* orbitals, being perpendicular to this plane, are denoted as the $\pi_{\perp}$ and $\pi_{\perp}^*$ orbitals.

(38) Mulliken populations given in Table II are obtained at the HF level. This seems reasonable, since the interaction between $RhCl(AsH_3)_4$ and the distorted CO_2 would be discussed, semiquantitatively at least, on the HF level. Furthermore, a preliminary SD–CI study of Rh(I)–CO_2 shows that the maximum change in Mulliken AO populations due to electron correlation effect is less than 10^{-3}.[39]

(39) The geometry of Rh–CO_2 was taken to be the same as in the Rh–CO_2 core of $RhCl(AsH_3)_4(CO_2)$ and the same basis sets were used as in this work. The SD–CI calculation was carried out with the MELD program written by E. R. Davidson and his collaborators in University of Washington. A total of 17 173 spin-adapted configurations were examined with the perturbation selection (threshold = 10^{-4} hartree), and the resultant 4029 spin-adapted configurations were used in the variational SD–CI calculation. The contribution of main configuration was 0.93.

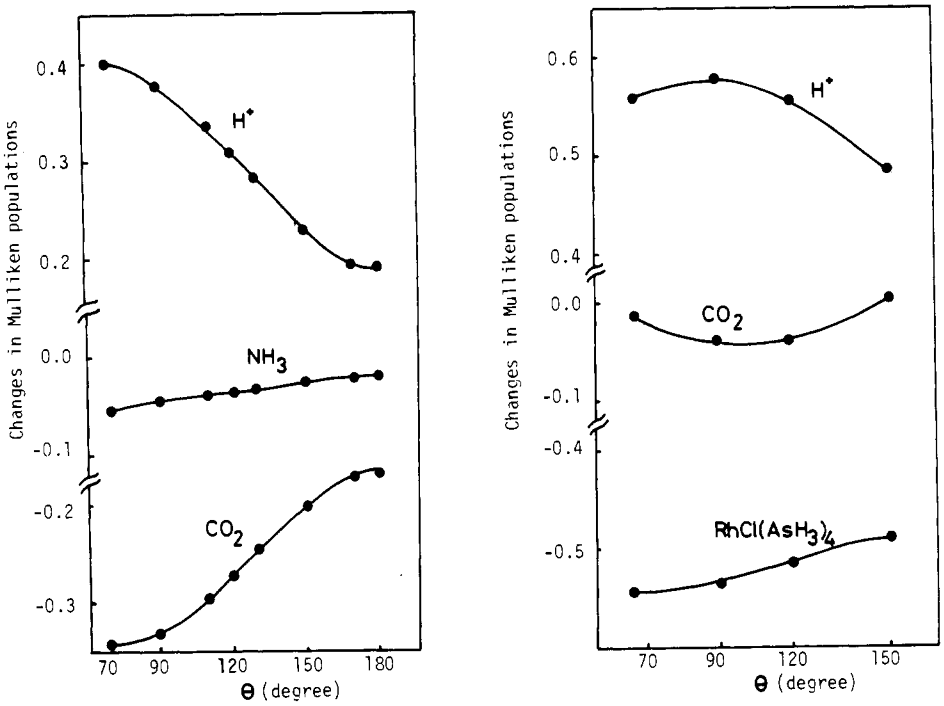

Figure 4. Changes in Mulliken populations caused by H^+ attack to coordinated CO_2. A positive sign means an increase in Mulliken population, and a negative sign means a decrease. R(Rh–C) = 2.02 Å (experimental).

electron population of carbon dioxide. In the $^3T_1$ state, similar but smaller changes in the Mulliken populations take place. This interaction stabilizes the $13a_1$ orbital, increases the energy difference between the $13a_1$ and $6b_2$ orbitals, as shown in Figure 2, and makes the ^1S state the most stable. Coordination of NH_3, however, remarkably raises the Rh d_{z^2} orbital energy but hardly changes the Rh $d_{x^2-y^2}$ orbital energy. This result is easily understood by considering that NH_3 has a lone-pair orbital but does not have any good acceptor orbital available for effective charge-transfer interaction. Certainly, the electron populations of NH_3 and the Rh d_{z^2} orbital are hardly influenced by NH_3 coordination (see Table II). Therefore, the Rh d_{z^2} orbital causes only a four-electron destabilizing interaction with the doubly occupied lone-pair orbital of NH_3, and the d_{z^2} orbital energy is significantly pushed up by NH_3 coordination. Consequently, the energy difference between Rh d_{z^2} and $d_{x^2-y^2}$ orbitals decreases upon NH_3 coordination, which makes the $^3T_1$ state the most stable.

Electrophilic Attacks of H^+ and CH_3^+ on the η^1-C-Coordinated CO_2. The attacks of H^+ and CH_3^+ on the coordinated carbon dioxide will be theoretically studied. Since we are interested in a qualitative conclusion, the reaction course of electrophilic attack was not optimized but electrophiles such as H^+ and CH_3^+ were placed rather arbitrarily at 1.5 and 2.0 Å from the oxygen atom, respectively (see Chart III) and the θ angle was varied only in the case of the H^+ attack. The stabilization energy resulted from the H^+ attack is given as a function of θ in Figure 3. While the stabilization energy by the H^+ attack is slightly larger at the MP2 level than at the HF level, both HF and MP2 methods result in very similar dependences of stabilization energy on the θ value. It is also noted that the stabilization energy in $(NH_3)(CO_2)\leftarrow H^+$ is about half of that in $RhCl(AsH_3)_4(CO_2)\leftarrow H^+$ at both the HF and the MP2 levels. The best value of θ is about 120° in $(NH_3)(CO_2)\leftarrow H^+$ and about 90° in $RhCl(AsH_3)_4(CO_2)\leftarrow H^+$. In $RhCl(AsH_3)_4(CO_2)\leftarrow H^+$, the electron population of H^+ is the greatest and that of CO_2 is the smallest around θ = 90°, as shown in Figure 4,[40] which suggests that the charge transfer from CO_2 to H^+ reaches a maximum around θ = 90°. In $(NH_3)(CO_2)\leftarrow H^+$, the charge transfer from CO_2 to H^+ becomes stronger with decreasing θ, whereas the stabilization energy is the largest around θ = 120°. These results suggest that the charge-transfer interaction plays a key role in the H^+ attack to $RhCl(AsH_3)_4(CO_2)$ but a different interaction is important in the $(NH_3)(CO_2)$ system. A candidate for such an interaction is the electrostatic interaction between CO_2 and H^+. A free CO_2 molecule has a quadruple moment of -4.2×10^{-26} cgsu, and consequently the electrostatic interaction favors the H^+ attack from the O end, as shown in Chart IV. The situation would be similar in $(NH_3)(CO_2)$ where geometrical and populational changes caused by the CO_2 coordination is remarkably small. Probably, the best θ value of 120° is a result of balance between the charge transfer and the electrostatic interactions.

Chart IV

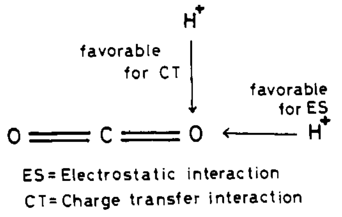

ES = Electrostatic interaction
CT = Charge transfer interaction

Table III. Attack of CH_3^+ on Coordinated CO_2 in $RhCl(AsH_3)_4(CO_2)$ and $(NH_3)(CO_2)^a$

	$RhCl(AsH_3)_4(CO_2)$		$(NH_3)(CO_2)$	
	θ = 90°	θ = 120°	θ = 90°	θ = 120°
ΔE kcal/mol	-64.7	-81.5	5.7	-9.6
changes in Mulliken pop.^{c}				
Rh or N	0.004	0.004	0.041	0.039
CO_2	-0.031	-0.008	-0.254	-0.189
AsH_3	-0.098	-0.093		
Cl	-0.117	-0.113		
CH_3^+	0.798	0.453	0.284	0.212

^{a}See Chart III for θ. R(Rh–C) = 2.02 Å and R(N–C) = 2.87 Å. The CH_3^+ was placed at a 2.0-Å distance from the oxygen atom. ^{b}The negative value means the stabilization in energy resulting from the CH_3^+ attack, and vice versa. ^{c}The positive value means an increase in Mulliken population upon CH_3^+ attack, and vice versa.

Since CH_3^+ is considered a more realistic model as an electrophile than H^+, the CH_3^+ attack to the coordinated CO_2 in

---

[40] Again, Mulliken populations at the HF level were used for this discussion, by considering the following results: (1) the stabilization energy by H^+ attack is only slightly larger at the HF level than at the MP2 level, and (2) both MP2 and HF methods result in a very similar dependence of stabilization energy on the θ value.

Chart V

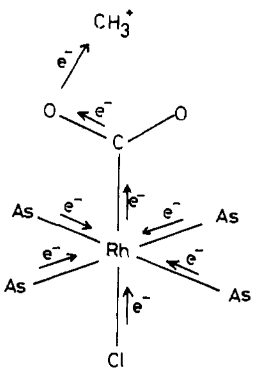

Chart VI

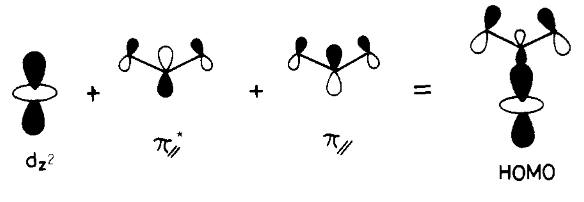

$RhCl(AsH_3)_4(CO_2)$ and $(NH_3)(CO_2)$ was examined at $\theta = 90°$ and 120°. The stabilization energy caused by the CH_3^+ attack is large in $RhCl(AsH_3)_4(CO_2)\leftarrow CH_3^+$, but very small in $(NH_3)(CO_2)\leftarrow CH_3^+$, as shown in Table III. Changes in Mulliken populations, given in Figure 4 and Table III,[40] exhibit interesting differences between these two reaction systems. First, the increases in electron populations of H^+ and CH_3^+ are much larger in the $RhCl(AsH_3)_4(CO_2)$ system than in the $(NH_3)(CO_2)$ system. Second, the CO_2 moiety loses little electron density upon electrophilic attack in the $RhCl(AsH_3)_4(CO_2)$ system, but it loses a lot in the $(NH_3)(CO_2)$ system. Third, electron populations of AsH_3 and Cl ligands decrease upon the CH_3^+ attack. All these results suggest that the charge-transfer interaction from CO_2 to an electrophile is much larger in the $RhCl(AsH_3)_4(CO_2)$ system than in the $(NH_3)(CO_2)$ system and that electrons transferred from CO_2 to the electrophile are efficiently supplied by Rh but are not effectively supplied by NH_3. Nevertheless, the atomic population of Rh slightly increases upon electrophilic attack, because electrons are again supplied to Rh by AsH_3 and Cl ligands. This redistribution of electrons is summarized in the schematical picture in Chart V. Such an electron flow is difficult in $(NH_3)(CO_2)$, and consequently, the reactivity of CO_2 coordinated with $RhCl(AsH_3)_4$ is much more enhanced than that in $(NH_3)(CO_2)$. This difference between $(NH_3)(CO_2)$ and $RhCl(AsH_3)_4(CO_2)$ is discussed later.

Electronic Structure of Coordinated Carbon Dioxide. Finally, the enhanced reactivity of coordinated carbon dioxide is discussed in relation to the coordinate bond of carbon dioxide. The difference density map $\{=\rho[RhCl(AsH_3)_4(CO_2)] - \rho[RhCl(AsH_3)_4] - \rho[CO_{2\,dist}]\}$ (dist = the distorted structure) given in Figure 5A offers clear features of electron distribution:[38-40] First, electron density substantially decreases in the regions of the Rh d_{z^2} orbital and the trans-positioned Cl ligand and remarkably increases in the region of carbon dioxide. Second, the electron density does not increase much on the carbon atom but increases very much on the oxygen atom. In Figure 5B, a contour map of the HOMO of $RhCl(AsH_3)_4(CO_2)$ is pictured. In this orbital, the oxygen p_π contribution is much larger than the carbon p_π contribution, which reflects the abovementioned electron distribution. This feature of HOMO is easily explained in terms of a mixing of three orbitals, Rh d_{z^2}, CO_2 $\pi_\parallel$ and $\pi_\parallel^*$ orbitals, as shown in Chart VI; the CO_2 $\pi_\parallel^*$ orbital overlaps in a bonding phase with the HOMO of $RhCl(AsH_3)_4$ which mainly consists of the Rh d_{z^2} and Cl p_z orbitals. Into this bonding overlap, the CO_2 $\pi_\parallel$ orbital mixes in an antibonding phase with the Rh d_{z^2} orbital. Consequently, this mixing increases the oxygen p_π contribution but reduces the carbon p_π contribution to the HOMO, leading to the significant increase in electron density around the oxygen atoms.

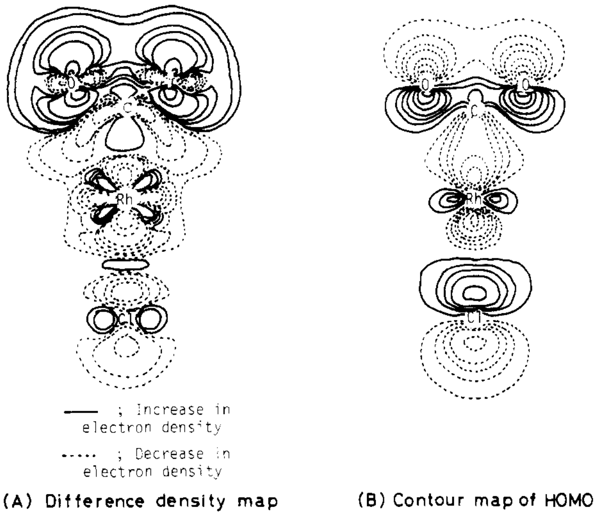

Figure 5. Difference density map and contour map of the HOMO in $RhCl(AsH_3)_4(CO_2)$. (A) Difference density = $\rho[RhCl(AsH_3)_4(CO_2)] - \rho[RhCl(AsH_3)_4] - \rho[CO_2]$ ±0.1, ±0.05, ±0.005, ±0.001, ±0.0005, ±0.0003. (B) Contour map: ±0.25, ±0.20, ±0.15, ±0.10, ±0.075, ±0.050, ±0.025. R(Rh–C) = 2.02 Å (experimental).

An enhancement of reactivity of the η^1-C-coordinated carbon dioxide is also explained by the above-described orbital mixing of HOMO. When the electrophilic attack to the oxygen atom is a charge-control reaction, the reactivity of coordinated carbon dioxide is expected to be enhanced very much, because the electron density of the oxygen atom is significantly increased by the η^1-C-coordination of carbon dioxide. When the electrophilic attack proceeds under frontier control, the energy level and the composition of HOMO are important. In the free molecule of CO_2, HOMO is a nonbonding π ($n\pi$) orbital and is positioned at −14.6 eV. the CO_2 coordination with $RhCl(AsH_3)_4$ raises the energy levels of $n\pi_\parallel$ and $n\pi_\perp$ orbitals to −10.2 and −10.4 eV, respectively, probably owing to electron accumulation on the oxygen atoms that is induced by the strong charge-transfer interaction from Rh to CO_2. Furthermore, the HOMO of $RhCl(AsH_3)_4(CO_2)$, lying at −8.1 eV, contains a large p_π orbital of oxygen atoms arising from the orbital mixing of Chart VI. Thus, it is reasonably concluded that the strong charge-transfer interaction also enhances the frontier-controlled electrophilic attack to the oxygen atom in the η^1-C-coordinated CO_2 complex.

The electronic structure of coordinated carbon dioxide can be compared in $RhCl(AsH_3)_4(CO_2)$ and $(NH_3)(CO_2)$, since the reactivity of the former is much more enhanced than that of the latter in spite of both having the same η^1-C-coordinated carbon dioxide. Coordination of carbon dioxide with NH_3 only slightly increases the electron population of carbon dioxide, as shown in Table II, and the binding energy of carbon dioxide with NH_3 is only 4.8 kcal/mol on the HF level and 4.7 kcal/mol on the MP2 level. The HOMO of this complex is the lone pair of NH_3, which is much lower in energy than that in $RhCl(AsH_3)_4$ and mixes very little with the $\pi_\parallel^*$ orbital of carbon dioxide. These are reasons why the distortion of coordinated carbon dioxide is very small, as depicted in Figure 1. At the same time, the coordination of CO_2 with NH_3 only slightly raises the energy level of the $n\pi$ orbital (−13.8 eV) and causes little contribution from the oxygen p_π orbital to the HOMO. Thus, the very weak charge-transfer interaction from NH_3 to CO_2 is the reason that carbon dioxide in $(NH_3)(CO_2)$ exhibits much less reactivity than carbon dioxide in $RhCl(AsH_3)_4(CO_2)$.

Conclusions

The ground state of $RhCl(AsH_3)_4(CO_2)$ is calculated to be a singlet, despite the fact that it has a pseudooctahedral d^8 electron configuration. On the other hand, $RhCl(AsH_3)_4(NH_3)$ is calculated to have a d–d triplet ground state, as one might expect. This difference between $RhCl(AsH_3)_4(CO_2)$ and its NH_3 analogue reflects the characteristic feature of carbon dioxide ligand. The η^1-C-coordinating carbon dioxide is a Lewis acid and accepts electrons from the Rh d_{z^2} orbital through the strong bonding interaction between CO_2 $\pi_{\parallel}{}^*$ and Rh d_{z^2} orbitals, leading to significant stabilization of the Rh d_{z^2} orbital. On the other hand, the NH_3 ligand has a lone pair and is a typical Lewis base, which destabilizes the doubly occupied d_{z^2} orbital with a four-electron destabilizing interaction between these two orbitals. $RhCl(AsH_3)_4(CO_2)$ can be viewed as a charge-transfer complex between carbon dioxide and $RhCl(AsH_3)_4$, because of a significant charge transfer from Rh to carbon dioxide. Such a significant charge-transfer interaction accumulates electrons on the terminal oxygen atoms. Simultaneously, this interaction raises the energy level of π and $n\pi$ orbitals of carbon dioxide and increases the oxygen p_π contribution to the HOMO originating mainly from the Rh d_{z^2} orbital. Consequently, the electrophilic attack to the oxygen atom of CO_2 is much enhanced in $RhCl(AsH_3)_4(CO_2)$. On the other hand, little charge transfer occurs in $(NH_3)(CO_2)$, where the complexed carbon dioxide is much less reactive with an electrophile than the carbon dioxide of $RhCl(AsH_3)_4(CO_2)$.

Acknowledgment. S.S. gratefully acknowledges the support of the Japanese Ministry of Education, Culture, and Science through Grant-in-Aids for Scientific Research (Nos. 60540306 and 62303002). Calculations were carried out at the Computer Center, Institute for Molecular Science (IMS), through the joint-study program of IMS.

Registry No. $RhCl(AsH_3)_4(CO_2)$, 117828-06-5; $RhCl(AsH_3)_4(NH_3)$, 117828-07-6; $RhCl(AsH_3)_4$, 117828-08-7; NH_3, 7664-41-7; CO_2, 124-38-9.

Contribution from the Gibbs Chemical Laboratory, Harvard University, Cambridge, Massachusetts 02138,
Quantum Theory Project, Departments of Chemistry and Physics, University of Florida,
Gainesville, Florida 32611, and Department of Chemistry, Auburn University, Auburn, Alabama 36849

Electron Correlation Effects on the Ground-State Structure and Stability of Triborane(9)

John F. Stanton,[†,‡] William N. Lipscomb,*[,‡] Rodney J. Bartlett,[§,‖] and Michael L. McKee[⊥]

Received May 18, 1988

Coupled-cluster and many-body perturbation (MBPT) theories are applied to a study of the ground-state structure and thermodynamic stability of triborane(9). Electron correlation effects are shown to have a dramatic influence on the predicted equilibrium structure of B_3H_9, shortening the nominally nonbonded B···B distances by 0.15 Å relative to the minimum-energy self-consistent-field structure. Reaction energies for $B_2H_6 + BH_3 \rightarrow B_3H_9$ are also sensitive to correlation effects, which stabilize the product by approximately 20 kcal/mol. For a [4s3p1d]/[3s1p] Gaussian basis set, the MBPT(4) electronic reaction energy is −7.9 kcal/mol. Introduction of thermal and entropic effects, however, favors the reactants. At room temperature, the Gibbs free energy change for the reaction is predicted to be +4.6 kcal/mol, suggesting that B_3H_9 does not serve to trap BH_3 during the pyrolysis of diborane.

Introduction

Although triborane(9) (see Figure 1) has not been characterized experimentally, its formation and subsequent destruction are believed to play an important role in the pyrolysis of diborane (B_2H_6). The mechanism for this important sequence of reactions, which served as the original synthetic route to the higher boranes,[1] has not been unambiguously determined. It is widely believed, however, that the process is initiated by the three elementary reactions[2]

$$B_2H_6 \rightleftharpoons 2BH_3 \tag{1}$$

$$BH_3 + B_2H_6 \rightleftharpoons B_3H_9 \tag{2}$$

$$B_3H_9 \rightleftharpoons B_3H_7 + H_2 \tag{3}$$

with either step 2 or 3 rate-limiting. The ephemeral existence of a triboron hydride has been supported by mass spectroscopy,[3] but no thermochemical or kinetic information pertaining to reactions 2 and 3 exists. Consequently, ab initio calculations appear to provide the most suitable means for studying this important process. Here too, however, the boranes present a problem. The quasi degeneracy of the boron 2s and 2p atomic orbitals leads to a number of configurations that make important contributions to the exact molecular wave function. Hence, the simple molecular orbital description is not suitable for *quantitative* theoretical studies of this class of compounds. Recent advances in quantum-chemical theory and computational speed have made the calculation of highly correlated molecular wave functions routinely possible for small to moderately sized systems. In the past few years, we have carried out large-scale calculations on a number of electron-deficient molecules, including BH_3 and B_2H_6,[4] B_2H_4,[5] and BeB_2H_8.[6] Currently, our efforts are directed toward application of these techniques to the diborane pyrolysis mechanism. In this paper, we report results of recent calculations on the ground-state structure and energy of triborane(9), a molecule that has proven to be unusually sensitive to electron correlation effects.

Calculations

Calculations reported here were carried out with the ACES program system, developed by Bartlett and collaborators.[7] Two basis sets have been used in this study: the fully polarized [3s2p1d]/[2s1p] and [4s3p1d]/[3s1p] sets used by Redmon, Purvis, and Bartlett[8] [hereafter termed (321/21) and (431/31)]. In addition, some calculations were performed with a basis derived from (321/21) by deleting the hydrogen polarization functions [(321/2)]. Unconstrained geometry optimizations of B_3H_9 (as well as B_2H_6 and BH_3) were performed with both basis sets at two levels of theory: the self-consistent-field (SCF) approximation and many-body perturbation theory,[9] carried out to second order [MBPT(2)]. At (321/21)-MBPT(2) equilibrium geometries, energy differences were calculated at a variety of highly correlated levels: MBPT through full

---

[†] AT&T Foundation Fellow. Present address: Department of Chemistry, The University of Chicago, Chicago IL.

[‡] Harvard University.

[§] Guggenheim Fellow, Harvard University, Fall 1986.

[‖] University of Florida.

[⊥] Auburn University.

(1) For an early history of the pyrolysis reactions, see: Hughes, R. L.; Smith, I. C.; Lawless, E. W. In *Production of the Boranes and Related Research*; Holzmann, R. T., Ed.; Academic Press: London, 1967.

(2) Fehlner, T. P. In *Boron Hydride Chemistry*; Mueterties, E. L., Ed.; Academic Press: New York, 1975, pp 185–187.

(3) Fridmann, S. A.; Fehlner, T. P. *J. Am. Chem. Soc.* **1971**, *93*, 2824; *Inorg. Chem.* **1972**, *11*, 936.

(4) Stanton, J. F.; Bartlett, R. J.; Lipscomb, W. N. *Chem. Phys. Lett.* **1987**, *138*, 525.

(5) Stanton, J. F.; Bartlett, R. J.; Lipscomb, W. N. In *IMEBORON VI Proceedings*; World Scientific Publishing: Singapore, 1988.

(6) Stanton, J. F.; Lipscomb, W. N.; Bartlett, R. J. *J. Chem. Phys.* **1988**, *88*, 5726.

(7) Bartlett, R. J.; Purvis, G. D.; Fitzgerald, G. B.; Harrison, R. J.; Lee, Y. S.; Laidig, W. D.; Cole, S. J.; Magers, D. H.; Salter, E. A.; Trucks, G. W.; Sosa, C.; Rittby, M.; Pal, S.; Stanton, J. F. "ACES (Advanced Concepts in Electronic Structure)—An *Ab Initio* Program System".

(8) Redmon, L. T.; Purvis, G. D.; Bartlett, R. J. *J. Am. Chem. Soc.* **1979**, *101*, 2856.

(9) Bartlett, R. J. *Annu. Rev. Phys. Chem.* **1981**, *32*, 359 and references therein.